

## A MOM-based algorithm for moving force identification: Part II – Experiment and comparative studies

Ling Yu

*Key Lab of Disaster Forecast and Control in Engineering, Ministry of Education of the People's Republic of China (Jinan University), Guangzhou 510632, P. R. China*  
*Department of Civil and Structural Engineering, The Hong Kong Polytechnic University*  
*Hong Kong, P. R. China*

Tommy H.T. Chan<sup>†</sup>

*School of Urban Development, Faculty of Built Environment & Engineering, Queensland University of Technology, GPO Box 2434, Queensland 4001, Australia*  
*Department of Civil and Structural Engineering, The Hong Kong Polytechnic University*  
*Hong Kong, P. R. China*

Jun-hua Zhu

*Key Lab of Disaster Forecast and Control in Engineering, Ministry of Education of the People's Republic of China (Jinan University), Guangzhou 510632, P. R. China*  
*Changjiang River Scientific Research Institute, Wuhan 430010, P. R. China*

*(Received August 30, 2006, Accepted August 7, 2007)*

**Abstract.** A MOM-based algorithm (MOMA) has been developed for moving force identification from dynamic responses of bridge in the companion paper. This paper further evaluates and investigates the properties of the developed MOMA by experiment in laboratory. A simply supported bridge model and a few vehicle models were designed and constructed in laboratory. A series of experiments have then been conducted for moving force identification. The bending moment and acceleration responses at several measurement stations of the bridge model are simultaneously measured when the model vehicle moves across the bridge deck at different speeds. In order to compare with the existing time domain method (TDM), the best method for moving force identification to date, a carefully comparative study scheme was planned and conducted, which includes considering the effect of a few main parameters, such as basis function terms, mode number involved in the identification calculation, measurement stations, executive CPU time, Nyquist fraction of digital filter, and two different solutions to the ill-posed system equation of moving force identification. It was observed that the MOMA has many good properties same as the TDM, but its CPU execution time is just less than one tenth of the TDM, which indicates an achievement in which the MOMA can be used directly for real-time analysis of moving force identification in field.

**Keywords:** moving force identification; method of moments (MOM); bridge loads; time domain method (TDM); dynamic responses.

---

<sup>†</sup> Ph.D., Corresponding author, E-mail: [tommy.chan@qut.edu.au](mailto:tommy.chan@qut.edu.au)

## 1. Introduction

The moving force identification is a fundamental problem in the bridge engineering (Olsson 1991). The importance of this problem has attracted much attention during the last two decades due to the large increase in the proportion of heavy vehicles and high-speed vehicles in highway and railway traffic (Yu and Chan 2005, Cebon 1987, Cantineni 1992). Accurate identification of moving forces during operation is vital for cost effective design and maintenance of bridges since this can not only lead to a great reliance on numerical simulation based upon analytical models but also dramatically reduce the need for more expensive and time consuming experimental testing (Chan and O'Conner 1990, Yu and Chan 2002).

In recent years, a series of identification methods have been successively proposed and merged into a moving force identification system (MFIS) (Yu 2002), and some further comparative studies on the effects of different parameters on the system have also been carried out and critically investigated in laboratory (Chan *et al.* 2000, Yu and Chan 2003), in which the time domain method (TDM) (Law *et al.* 1997) has been proved to be the best one in all of the identification methods and applied successfully to a field study (Chan *et al.* 2000). Although all these methods can identify moving forces with acceptable accuracy, each method has its own merits, limitations and disadvantages. For example, the TDM has higher identification accuracy but it is time consuming. Moreover, the TDM often provides a significant fluctuation at the beginning and the end of time histories of identified moving forces due to the nature of ill-posed problem of moving force identification (Tikhonov and Arsenin 1977, Santantamarina and Fratta 1998, Law *et al.* 2001).

Based on the method of moments (MOM) and the theory of moving force identification, a MOM-based algorithm (MOMA) has been proposed for identifying the time-varying vehicle axle loads from the dynamic responses of a bridge in the companion paper (Yu *et al.* 2008). Some numerical simulation results have shown that the MOMA has higher identification accuracy and robust noise immunity as well as an acceptable solution to the ill-conditioning problem to some extent. However, these results are all from the numerical simulation at all, and the best tool to assess the new method should be through experiments in laboratory or field tests (Harris and Sabnis 2000, Bilello *et al.* 2004).

As its companion paper (Yu *et al.* 2008), this paper aims to further evaluate and critically investigate the MOMA and compare it with the existing TDM through experiments in laboratory based on a comparative study. A bridge-vehicle system is designed and fabricated in laboratory, a series of experiments have been conducted for moving force identification under different conditions. The bending moment and acceleration responses at some measurement stations of the bridge model are simultaneously measured when the model vehicle moves across the bridge deck at different speeds. In contrast to the TDM, a carefully comparative study scheme was planned and conducted, which includes considering the effect of a few main parameters, such as basis function terms, mode number involved in the identification calculation, measurement stations, CPU execution time, Nyquist fraction of digital filter, and two different solutions to the ill-posed system equation of moving force identification. Some conclusions are finally made.

## 2. Experiments in laboratory

After the proposed MOMA method had been evaluated through numerical simulations in the

companion paper (Yu *et al.* 2008), a series of experiments were further conducted in laboratory for assessing the robustness of MOMA.

## 2.1 Experimental setup

Both the model car and model bridge deck were designed and fabricated in the laboratory as shown in Fig. 1. Here, a beam model was used to model the tested bridge and a car model was constructed from available materials in the laboratory. The model car had two axles at a spacing of 0.55 m and was mounted on four rubber wheels. The static mass of the whole vehicle was 12.1 kg in which the mass of the rear wheel was 3.825 kg. The model bridge deck consisted of a main beam, a leading beam and a trailing beam. The leading and trailing beam were attached at both ends of the main beam, in which the leading beam was used for initiating the motion and speeding up the car so that the car could reach a constant speed when it approaches the main beam. The trailing beam was used for decelerating the car. The main beam, with a span of 3.678 m long and a 101 mm × 25 mm uniform cross section, was simply supported. It was made from a solid rectangular mild steel bar with a density of 7335 kg/m<sup>3</sup> and a flexural stiffness  $EI = 29.97$  kN·m<sup>2</sup>. A U-shape aluminum track was glued to the upper surface of the main beam as a guide way for the model-car. The first three theoretical natural frequencies of the main beam bridge were calculated as 4.5 Hz, 18.6 Hz and 40.5 Hz respectively. The tested bridge model is fabricated, as shown in Fig. 2.

Sensors used in the experiments include photoelectric sensors, strain gauges and accelerometers. Seven photoelectric sensors were mounted beside the beams to measure and check the uniformity of the moving speed of the model car. Seven strain gauges and three accelerometers were equally spaced mounted on the lower surface of the main beam to measure the bridge response when the model car was moving across it. A system calibration of the strain gauges was carried out before the actual testing program by adding masses at the middle of the main beam. The calibration factors for each of the strain gauges are listed in Table 1.

A data acquisition system was prepared to acquire the dynamic responses of the bridge model induced by the model car crossing the bridge. The system comprises of a sensor element, a conditioning element, a converting element and a processing element. During the test, the model car was pulled along by a string wound around the drive wheel of an electric motor. The speed of the motor could be adjusted in order to get a specific car speed. A 14-channel tape recorder was employed to record the response signals. The first seven channels were used for logging the bending moment response signals from the strain gauges, channels 8-10 were for the acceleration response signals from the accelerometers, and channel 11 was connected to the photoelectric sensors. In addition, the response signals from channels 1-7 and 11 were also recorded simultaneously into a PC for easy analysis in situ. The software Global Lab from the Data Translation was used for data acquisition and analysis in the laboratory tests. Under all the studied cases, the data were acquired

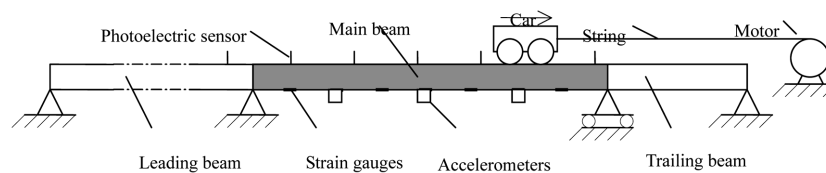


Fig. 1 Experimental model designed for laboratory tests

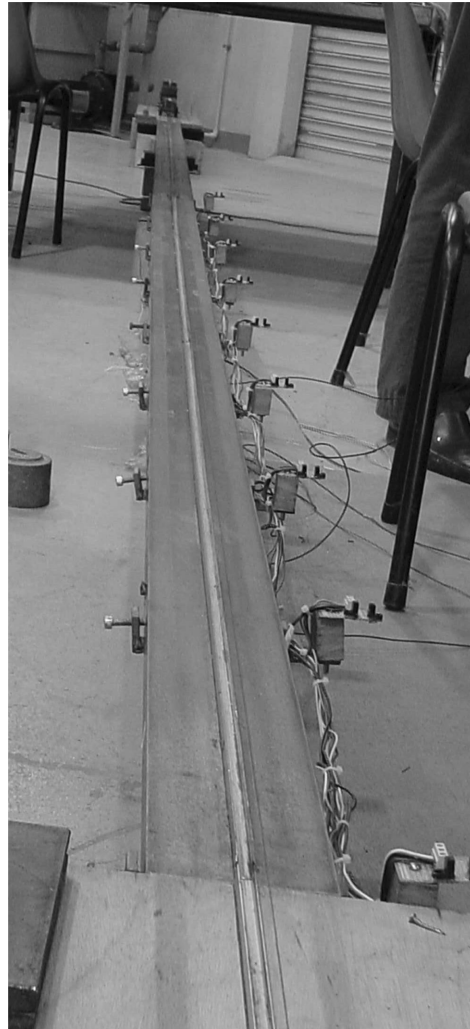


Fig. 2 Experimental model fabricated in the laboratory

Table 1 Calibration factors of strain gauges

Station no.	Channel no.	Strain gauge no.	Location in span (L)	Calibration factor (Nm/V)
1	1	1	1L/8	289.0
2	2	2	2L/8	285.2
3	3	3	3L/8	285.9
4	4	4	4L/8	296.6
5	5	5	5L/8	297.7
6	6	6	6L/8	297.1
7	7	7	7L/8	298.4

in a sampling frequency of 1000 Hz, which is higher than the practical demands. The data sequences were sampled again to form a new sequence at a lower sampling frequency. When deciding the sampling frequency to form a new data sequence, the new sampling was checked if it fulfilled the Nyquist rate requirement (Proakis and Manolakis 1996). Before exporting the measured data in ASCII format for identification, the Bessel IIR digital filter with low-pass characteristics was implemented as cascaded second order systems. The Nyquist fraction value was chosen to be 0.03 and 0.05 respectively for different requirement of frequency band needed.

## 2.2 Experimental results

The measured bending moment and acceleration responses of the bridge were recorded under three sets of vehicle speed, i.e., 5, 10 and 15 Units. After acquiring the data, the vehicle speed was calculated and the uniformity of the speed was checked. If the speed was stable, the experiment was repeated five times under each speed case to check whether the properties of both the structure and the measurement system had changed or not. If no significant change was found, the corresponding recorded data was accepted for identification of the moving forces. The identification of each case and check of the uniformity of vehicle speed is shown in Table 2.

All the response data recorded into the PC and the Tape recorder under each case were checked and found that they were all very good and could be used to identify the moving forces on the bridge. Two typical measured responses of bending moments at seven equally spaced strain gauges and acceleration responses at three equally spaced accelerometers, which were installed on the lower surface of the bridge, are plotted in Fig. 3. All filtered data corresponding to all scheduled cases were stored in the personal computer and exported in ASCII format for moving force identification in two-force study cases.

Table 2 Experimental measurement cases and vehicle speed calculation

Cases		Speed of vehicle at different segments of bridge span (m/s)					
Speed	Name	1	2	3	4	5	Average
5 Unit	U5-1	0.6975	0.7197	0.7226	0.7084	0.7130	0.71224
	U5-2	0.7208	0.7340	0.7000	0.7029	0.7267	0.71688
	U5-3*	0.7073	0.7524	0.7312	0.7205	0.7148	0.72524
	U5-4	0.754	0.7569	0.7246	0.7186	0.7201	0.73484
	U5-5	0.7306	0.7417	0.7105	0.7038	0.6992	0.71716
10 Unit	U10-1	1.2715	1.3978	1.4690	1.5124	1.2921	1.38856
	U10-2	1.4067	1.2073	1.0063	1.1002	1.1393	1.17196
	U10-3	1.1968	1.1478	1.1058	1.1204	1.1158	1.13732
	U10-4	1.0943	1.0939	1.0719	1.0598	1.1144	1.08686
	U10-5	1.1407	1.1354	1.1073	1.1113	1.1003	1.11900
15 Unit	U15-1	1.4755	1.5417	1.4935	1.4718	1.5372	1.50394
	U15-2	1.505	1.5267	1.5132	1.5421	1.5291	1.52322
	U15-3	1.2463	1.2656	1.2798	1.2650	1.2386	1.25906
	U15-4	1.6793	1.7424	1.7692	1.7426	1.5318	1.69306
	U15-5	1.5202	1.5608	1.5815	1.5082	1.5594	1.54602

\*Notes: Case U5-3 means the third test when the vehicle runs at the speed of 5 Unit.

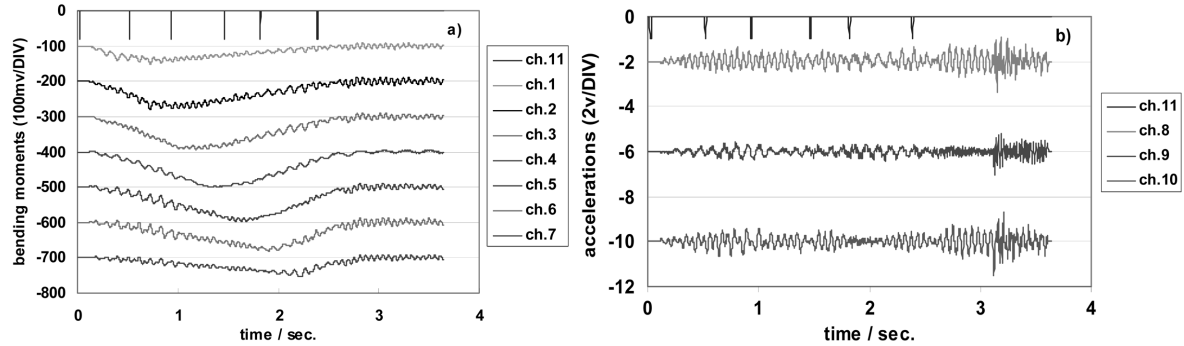


Fig. 3 Typical measured responses of bridge due to moving vehicle

### 3. Comparative studies

The moving force identification includes many parameters, which are the critical parts in the identification processing. The comparative study is to investigate the effects of several main parameters on the MOMA, and further compared with the existing TDM. The parameters studied include basis function terms, mode number, measurement stations, CPU execution time, the Nyquist fraction value, and various solutions to the ill-posed problem of system equation on the moving force identification (Yu *et al.* 2008). For practical reasons, the parameters were studied one at a time. The procedure was to examine each parameter in studied cases and to isolate the case with the highest accuracy for the corresponding parameter.

#### 3.1 Accuracy assessment

As the true moving forces are unknown in practice, the identification accuracy of moving forces cannot be evaluated directly, but can be assessed indirectly through the measured and rebuilt responses. The latter are calculated from the identified moving forces as a forward problem in the structural dynamics. Therefore, the accuracy, called relative percentage error (RPE), is quantitatively defined as below

$$RPE = \frac{\sum |R_{measured} - R_{rebuilt}|}{R_{measured}} \times 100\% \quad (1)$$

Here,  $R_{measured}$  indicates the measured response and  $R_{rebuilt}$  the rebuilt response respectively.

In the comparative studies being reported here, the results were based on the measurements of bending moments. The results associated with the measured accelerations will be reported separately. The identified forces were first calculated from the bending moment responses at all seven measuring stations. The rebuilt responses were then computed accordingly from the identified forces. The RPE values between the rebuilt and measured bending moment responses at each station were finally tested for validation. The maximum acceptable RPE value adopted here is 10% (Chan *et al.* 2000).

### 3.2 Effect of basis function terms

Basis function plays an important role in the identification of moving loads for the MOMA. To assess the effect of basis function number (*BFN*) on the MOMA, the other parameters are chosen as following: the mode number of the bridge involved in the moving force identification is equal to four ( $MN = 4$ ), the sampling frequency is equal to 200 Hz ( $f_s = 200$  Hz), the speed of vehicle is 15 Units (*case* U15-2 in Table 2,  $c = 1.52322$  m/s), and the measurement bending moments at seven stations are all selected, i.e. the sensor number of locations are seven ( $N_l = 7$ ). Fig. 4 plots the effect of *BFN* on the MOMA with Legendre basis function and one with Fourier basis function, in which the *BFN* increases up to 600, while other parameters  $MN = 4$ ,  $f_s = 200$ ,  $c = 15$  Units,  $N_l = 7$  were not changed for any of the cases.

Fig. 4 illustrates that both the *RPE* values tend to be reduced and finally to be close to each other when *BFN* increases. The major difference between them is that the rate of reduction is obviously different. If the Fourier basis functions are used, the *RPE* values are dramatically reduced to the lowest value and then kept the lowest constant after the basis function term is equal to about 100 or more for each case. However, if the Legendre basis functions are adopted, the process of *RPE* reduction will be clearly slower than the Fourier case. It is noted that the identification accuracy is stable and kept the highest when the corresponding basis function terms are increased up to be more than 400, even 500.

Fig. 5 gives a comparison on the time histories of moving forces identified by the TDM and

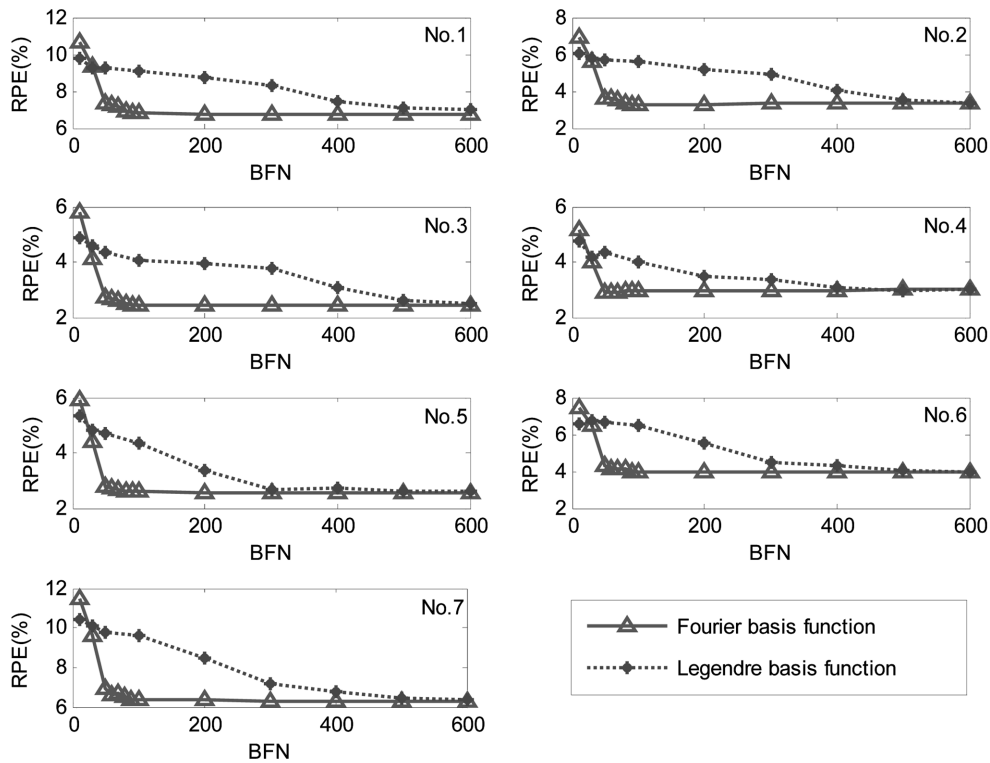


Fig. 4 Effect of basis function number (*BFN*) on MOMA

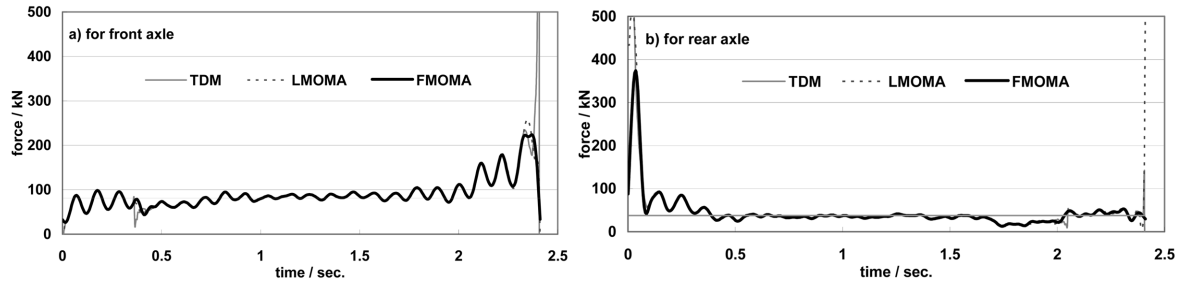


Fig. 5 Comparison on moving forces identified by TDM and MOMA

Table 3 Comparison of TDM and MOMA

Method	Station						
	1	2	3	4	5	6	7
TDM	6.72	3.31	2.43	2.99	2.58	3.96	6.29
MOMA	6.82	3.29	2.44	2.96	2.59	3.97	6.33

MOMA respectively when the basis function terms are equal to 500 for Legendre polynomials and 100 for Fourier series respectively. Here, the LMOMA result is from the MOMA when the basis function is Legendre polynomials. Similarly, the FMOMA result is from the basis function of Fourier series. From the figure, it can be seen that the identified results from the MOMA are in agreement with the TDM results. Moreover, the MOMA results are better than the TDM results, particularly for the moment at the beginning and the end of time history of two moving forces as well as the moment at the accessing and exiting of the vehicle on the bridge. For the front axle in Fig. 5(a), the moment of the second axle of the vehicle accessing into the bridge is at about 0.35 second, the TDM result has a big jump, but the MOMA result is smoother and better than the TDM. At the end of time history of the moving force at the front axle, the FMOMA is better than the LMOMA and both of them are further better than the TDM result since the FMOMA result does not result in an unreasonable jump. For the rear axle in Fig. 5(b), similarly, at about 2.05 second, the exiting moment of the front axle of the vehicle, the MOMA result is better than the TDM. At the beginning of time history of identified moving force at the rear axle, the FMOMA is better than the LMOMA and further better than the TDM. It can draw a conclusion from above that the MOMA can provide a more reasonable and acceptable solution to the ill-posed problem of the moving force identification to some extent when the MOMA is adopted to identify the moving forces from the bridge responses, especially for the FMOMA, the MOMA with the basis function of Fourier series.

Further, Table 3 lists the *RPE* values of the MOMA and the TDM respectively. It shows that the identification accuracy of the MOMA is consistent with that of the TDM. In addition, when the Fourier basis function is adopted, the FMOMA forms a coefficient matrix with a small dimension in the system equation and results in a small CPU execution cost due to the small *BFN*, so the MOMA has higher computation efficiency. Therefore, it is only considered the solutions of MOMA with Fourier basis function (FMOMA) in the following studies, from the point of view of computation efficiency as well as the identification accuracy.

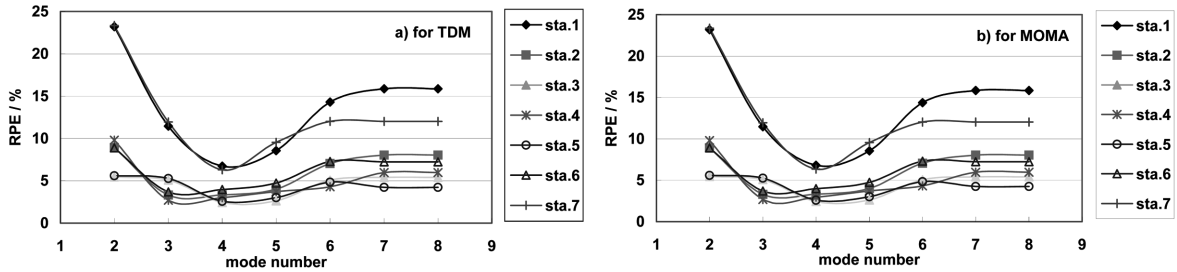


Fig. 6 Effect of mode number (MN) on TDM and MOMA

### 3.3 Effect of mode numbers

For both the TDM and MOMA, the case of  $f_s = 200$  Hz,  $c = 15$  Units,  $N_l = 7$  was chosen and not changed. The mode number was varied from  $MN = 2$  to  $MN = 8$ . Fig. 6 plots typical effects of the mode number on the two identification methods. Obviously, the effect of mode number on both MOMA and TDM is not so significant. With the mode number increase, the RPE curve decrease firstly and then increases, and the better case is  $MN = 4$  for both methods.

### 3.4 Effect of measurement stations

The case  $MN = 4$ ,  $f_s = 200$  Hz,  $c = 15$  Units is chosen for studying the effects of number and locations of measurement stations. The  $N_l$  were set to 3, 4, 5 and 7 respectively while other parameters were not changed for any cases. Table 4 lists a comparison on the RPE values by the TDM and MOMA respectively. It shows that there is no significant difference between the TDM and MOMA results for each case under the same condition. The effect of measurement stations on the MOMA is identical with that of TDM. In addition, Fig. 7 illustrates a comparison on the effect of measurement stations on the MOMA. It can be found that the more the number of measurement stations, the better the identified results for the MOMA as a general conclusion.

Table 4 Effect of Measurement Stations on TDM and MOMA

Statio	TDM				MOMA			
	$N_l = 3$	$N_l = 4$	$N_l = 5$	$N_l = 7$	$N_l = 3$	$N_l = 4$	$N_l = 5$	$N_l = 7$
1	*	*	*	6.72	*	*	*	6.82
2	*	1.58	2.37	3.31	*	1.58	2.37	3.29
3	1.50	1.95	2.16	2.43	1.50	1.95	2.15	2.44
4	1.67	*	2.87	2.99	1.71	*	2.88	2.96
5	1.71	2.26	2.45	2.58	1.70	2.26	2.44	2.59
6	*	1.69	2.33	3.96	*	1.69	2.35	3.97
7	*	*	*	6.29	*	*	*	6.33

Notes: Symbol \* indicates the station is not selected.

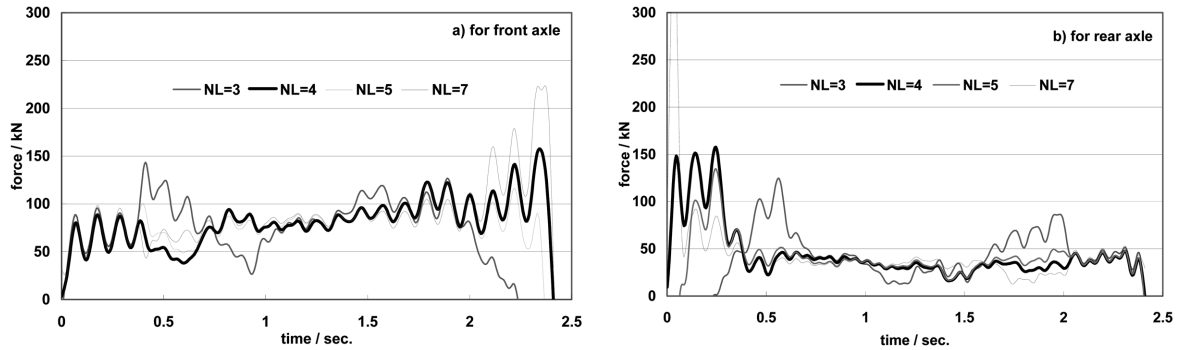


Fig. 7 Effect of measurement stations on moving forces for MOMA

Table 5 Comparison on executive CPU time (in second)

PART	TDM	MOMA
Forming coefficient matrix	18.219	19.907
Identifying moving forces	40.359	2.375
Rebuilding responses	1.063	1.094
Total	59.641	23.376

### 3.5 Comparison on CPU execution time

The CPU execution time consists of three parts for both TDM and MOMA, i.e. forming the system coefficient matrix, identifying moving forces and producing the rebuilt responses. The case described here is of  $MN = 4$ ,  $f_s = 200\text{Hz}$ ,  $c = 15$  Units,  $N_l = 7$  using a computer with Intel Pentium (R) 4 CPU 2.6GHz 512MB RAM. The total sampling points for bending moment responses at each measurement station are 560 and the total sampling points for each wheel axle force are 483 in the time domain. Therefore, the dimensions of coefficient matrix for TDM are  $(7 \times 560, 2 \times 483)$ , while the matrix for MOMA are  $(7 \times 560, 2 \times 101)$ . A detail comparison of the CPU execution time for each part of the TDM and MOMA is listed in Table 5. It shows that both the MOMA and TDM take almost the same time for both of the rebuilding responses and forming the system coefficient matrix. However, the CPU execution time of MOMA is about 6% of TDM for the identifying force process. Hence, the total consuming time of MOMA is only two fifth of that of TDM. Therefore, MOMA is a better and fast method, whether from the point of view of identifying force time or from the total consuming time. This advantage with higher computation efficiency for the MOMA is especially valuable for the on-line real-time analysis of moving force identification in situ.

### 3.6 Effect of nyquist fraction

To filter the high frequency noise of measured response signals, a Bessel IIR digital filter with low pass characteristics was chosen and implemented as a cascaded second order system. Different Nyquist fractions of the filter were chosen for the measured bending moments. The Nyquist fraction is defined as the ratio of cutoff frequency to sampling frequency of dynamic signals. The cutoff frequency may be specified in Hertz relative to the sampling frequency, or as a fraction of the

Table 6 Effect of Nyquist fractions on MOMA

Nyquist fraction	Station						
	1	2	3	4	5	6	7
0.03	6.72	3.31	2.43	2.99	2.58	3.96	6.29
	<u>6.82</u>	<u>3.29</u>	<u>2.44</u>	<u>2.96</u>	<u>2.59</u>	<u>3.97</u>	<u>6.33</u>
0.05	6.43	2.79	2.74	3.14	3.16	4.74	6.60
	<u>6.52</u>	<u>2.80</u>	<u>2.76</u>	<u>3.13</u>	<u>3.18</u>	<u>4.74</u>	<u>6.64</u>

Notes: the underlined values are from MOMA, others from TDM.

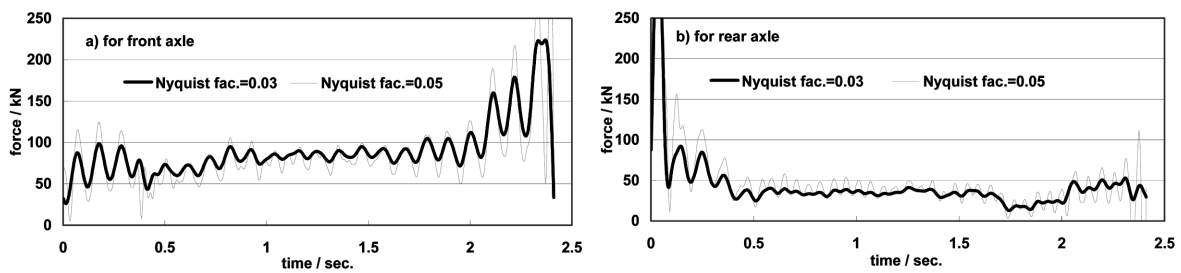


Fig. 8 Effect of Nyquist fractions on moving forces for MOMA

Nyquist frequency. A bigger Nyquist fraction indicates a filtered signal with higher frequency components in the frequency domain.

In this section, Nyquist fraction values were first set to 0.03 and 0.05 respectively and then used to filter the data samples recorded at the sampling frequency of 1000 Hz for all the cases. The new data sequence would be formed by sampling again at different rate, for example,  $f_s = 200$  Hz as required. To study the effect of Nyquist fraction on identification accuracy, only the Nyquist fraction was changed here, but others parameters  $MN = 4$ ,  $f_s = 200$  Hz,  $c = 15$  Units,  $N_l = 7$  were not changed for each case. Table 6 lists the RPE values when the Nyquist fraction changes for both TDM and MOMA respectively. It can be seen that the RPE values increases slightly with the increase in the Nyquist fraction whether from the TDM or MOMA results, which shows that the higher frequency noise has an influence on the identified results when the Nyquist fraction is set to be a higher value. Further, Fig. 8 illustrates the effect of Nyquist fractions on the identified moving forces for MOMA. It shows that the magnitude of identified forces increases and the identified forces have some clear higher frequency components when the Nyquist fraction has a higher value. Therefore, the Nyquist fraction should be selected properly to reasonably identify the moving vehicle loads on bridge.

### 3.7 Effects of different solutions

If the parameters  $MN = 4$ ,  $f_s = 200$  Hz,  $c = 15$  Units,  $N_l = 7$  were not changed for each case in this section, only two solutions, i.e., SVD and Regularization solutions, were adopted to solve the over-determined set of system equations respectively. Table 7 lists a comparison on the RPE values by both TDM and MOMA when the two solutions are adopted. It can be found from the Table 7

that the RPE values from each of two identification methods are increased a little bit when the Regularization solution is adopted in contrast to the SVD solution. This is because the SVD solution provides a solution to make the residual of  $Ax=b$  minimum for a system equation of  $Ax = b$ , but the Regularization solution provides a balance between the residual of  $Ax=b$  and the norm of  $x$ , i.e. it makes the summation of the residual and the norm minimum. So the Regularization solution is often not the minimum residual solution. When the system equation is ill-conditioning or there is noise in the response data vector of  $b$ , the SVD solution would be often unstable in the sense that small perturbations in the responses would result in large deviation from their true solution even a whole wrong solution (Law *et al.* 2001). However, the Regularization solution can be used to stabilize the unbounded solution since it provides a bound to the ill-posed problem on moving force identification.

Moreover, it can be seen from Table 7 that the regularization method has less influence on the TDM results in contrast to the MOMA results. Figs. 9 and 10 are the L-shape curves for selection of regularization parameters for TDM and MOMA respectively (Busby and Trujillo 1997, Hansen 1992, Hansen and O’Leavy 1993). From above two figures, it can be found that the regularization parameter is equal to 0.0096145 for the TDM but 0.16483 for the MOMA. The lower the regularization parameter, the better the fitting extent of solution to the responses, however, the less

Table 7 Comparison on RPE values by SVD and Regularization solutions

Methods	Station						
	1	2	3	4	5	6	7
TDM	6.72	3.31	2.43	2.99	2.58	3.96	6.29
	<u>6.73</u>	<u>3.31</u>	<u>2.43</u>	<u>2.99</u>	<u>2.58</u>	<u>3.95</u>	<u>6.30</u>
MOMA	6.82	3.29	2.44	2.96	2.59	3.97	6.33
	<u>7.08</u>	<u>3.29</u>	<u>2.47</u>	<u>2.76</u>	<u>2.67</u>	<u>3.82</u>	<u>6.75</u>

Notes: the underlined values are from Regularization solution, others from SVD solution.

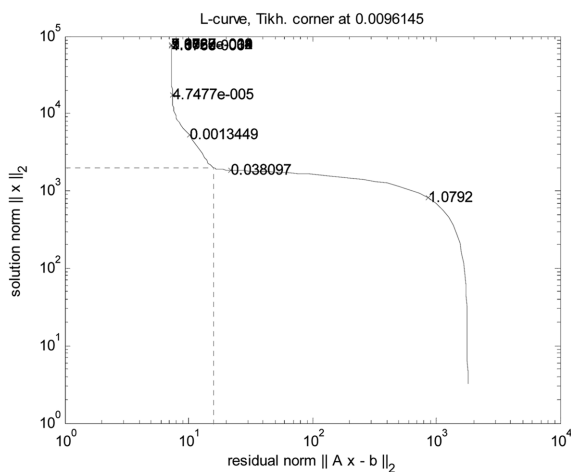


Fig. 9 L-shape curve for selecting regularization parameter for TDM

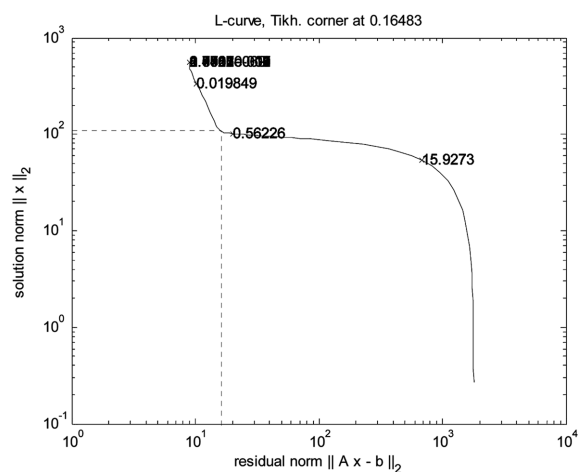


Fig. 10 L-shape curve for selecting regularization parameter for MOMA

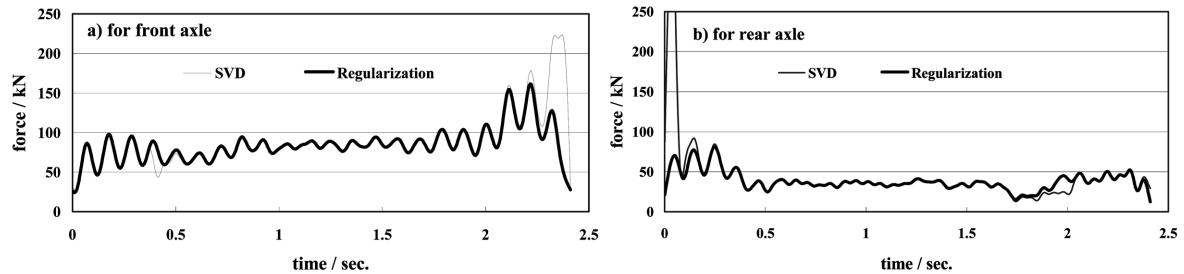


Fig. 11 Effect of two solutions on moving forces for MOMA

the bound constrains to the norm of solution. Therefore, the regularization method has a better efficiency to the MOMA than the TDM.

Fig. 11 illustrates a comparison on the identified moving forces due to the two solutions for MOMA. Basically, the regularization results are in agreement with the SVD results except for the moment at the beginning and the end of time histories of moving forces as well as the moment at the accessing and exiting of vehicle on bridge in the time history of moving forces. It shows that the fluctuation of identified moving forces can be effectively bounded at the moment mentioned above if the Regularization solution is adopted to solve the system equation for MOMA. The identified results by the Regularization solution are obviously improved. They are clearly better than the results by the SVD solution and more reasonable in practice.

#### 4. Conclusions

In this paper, a series of experiments have been carried out in the laboratory for evaluation on the MOM-based algorithm (MOMA), a new developed method for identification of moving forces from the responses of a bridge. A comparative study has been performed to assess the effect of some parameters on the new method using the measured data in laboratory. These parameters mainly include the basis function terms of both Legendre polynomials and Fourier series, mode number of bridge involved in the identification calculation, the measurement stations, the CPU execution time of identification method, Nyquist fraction of digital filter, and the two different solutions to the over-determined system equation. Some conclusions can be made as following. (1) The MOMA is correct, reasonable and suitable for moving force identification from the bridge responses. It is successful to identify the moving vehicle loads on bridges using the MOMA in laboratory. (2) Comparing with the existing time domain method (TDM), the MOMA has same good advantages as the TDM. Both the MOMA and TDM have similarly optimum selection criteria for the common parameters, such as mode number, measurement stations and Nyquist fraction. Some conclusions for the TDM are also suitable for the MOMA. (3) The basis function terms play an important role in the MOMA. The different patterns of basis function can lead to different computation efficiency, and the basis function number has been obviously affected the identification accuracy in practice. The more the basis function number is, the higher the MOMA identification accuracy is, but leading to longer CPU execution time. If the basis function number was chosen properly, the CPU time would be greatly shortened. Therefore, the basis function should be properly selected and appropriately determined in order to keep the MOMA more effective. (4) The MOMA can improve

the identification accuracy for the ill-posed problem on the moving force identification, but the fluctuation at the beginning and ending of time histories of identified moving forces are still significant. If the regularization solution is adopted to solve the over-determined system equation, the fluctuation mentioned above can be effectively bounded. (5) The MOMA has higher efficiency and better flexibility than the TDM. When the Fourier series are adopted as the basis function of the MOMA, the CPU execution time of MOMA is much less than the TDM. It is only about 6% of the TDM CPU execution time under the condition of keeping higher identification accuracy. The MOMA is obviously better than the TDM. When the regularization solution is adopted, the calculation cost will increase in contrast to the cost of the SVD solution, but the identification efficiency of the MOMA is still higher than that of SVD solution for the TDM, which is beneficial to the real-time analysis of moving loads identification in field. To conclude, as a feasible and reasonable identification method, the MOMA should be firstly recommended as a practical method of moving force identification in situ.

### Acknowledgements

The project is jointly supported by the National Natural Science Foundation of China (50378009), the Key Project of Chinese Ministry of Education of China (208172), the Foundation of Talent Program of Jinan University (51207052), the funding of the Key Lab of Diagnosis of Fault in Engineering Structures, Guangdong Province of the People's Republic of China (Jinan University), and the Hong Kong Polytechnic University Postdoctoral Fellowship Research Grants (G-YX25). The support by the Queensland University of Technology is also gratefully acknowledged.

### References

- Bilello, C., Bergman, L.A. and Kuchma, D. (2004), "Experimental investigation of a small-scale bridge model under a moving mass", *J. Struct. Eng.*, **130**(5), 799-804.
- Busby, H.R. and Trujillo, D.M. (1997), "Optimal regularization of an inverse dynamic problem", *Comput. Struct.*, **63**(2), 243-248.
- Cantineni, R. (1992), "Dynamic behavior of highway bridges under the passage of heavy vehicles", Swiss Federal Laboratories for Materials Testing and Research (EMPA) Report No. 220, 240.
- Cebon, D. (1987), "Assessment of the dynamic wheel forces generated by heavy road vehicles", Symposium on Heavy Vehicle Suspension and Characteristics, Austrian Road Research Board.
- Chan, T.H.T. and O'Conner, C. (1990), "Wheel loads from highway bridge strains: Field studies", *J. Struct. Eng.*, ASCE, **116**(7), 1751-1771.
- Chan, T.H.T., Law, S.S. and Yung, T.H. (2000), "Moving force identification using an existing prestressed concrete bridge", *Eng. Struct.*, **22**, 1261-1270.
- Chan, T.H.T., Yu, L. and Law, S.S. (2000), "Comparative studies on moving force identification from bridge strains in laboratory", *J. Sound Vib.*, **235**(1), 87-104.
- Hansen, P.C. (1992), "Analysis of discrete ill-posed problems by means of the L curve", *SIAM Rev.*, **34**, 561-580.
- Hansen, P.C. and O'Leavy, D.P. (1993), "The use of the L curve in the regularization of discrete ill-posed problems", *SIAM J. Sci. Comput. (USA)*, **14**, 1487-1503.
- Harris, H.G. and Sabnis, G.M. (2000), *Structural Modeling and Experimental Techniques*, CRC Press, New York.
- Law, S.S., Chan, T.H.T., Zhu, X.Q. and Zeng, Q.H. (2001), "Regularization in moving force identification", *J. Eng. Mech.*, ASCE, **127**(2), 136-148.

- Law, S.S., Chanm T.H.T. and Zeng, Q.H. (1997), "Moving force identification: A time domain method", *J. Sound Vib.*, **201**(1), 1-22.
- Olsson, M. (1991), "On the fundamental moving load problem", *J. Sound Vib.*, **145**(2), 299-307.
- Proakis, G.J. and Manolakis, D.G. (1996), *Digital Signal Processing, Principle, Algorithms and Applications*, Prentice-Hall Inc.
- Santantamarina, J.C. and Fratta, D. (1998), "Introduction to discrete signals and inverse problems in civil engineering", ASCE, Reston. Va., 200-238.
- Tikhonov, A.N. and Arsenin, V.Y. (1977), *Solution of Ill-posed Problems*. Wiley. New York.
- Yu, L. (2002), "Accounting for bridge dynamic loads using moving force identification system (MFIS)", Ph.D. Thesis, The Hong Kong Polytechnic University, Hong Kong.
- Yu, L. and Chan, T.H.T. (2002), "Moving force identification from bending moment responses of bridge", *Struct. Eng. Mech.*, **14**(2), 151-170.
- Yu, L. and Chan, T.H.T. (2003), "Moving force identification based on the frequency-time domain method", *J. Sound Vib.*, **261**, 329-349.
- Yu, L. and Chan, T.H.T. (2005), "Moving force identification from bridge dynamic responses", *Struct. Eng. Mech.*, **21**(3), 369-374.
- Yu, L., Chan, T.H.T. and Zhu, J.H. (2008), "A MOM-based algorithm for moving force identification: Part I – theory and numerical simulation", *Struct. Eng. Mech.*, **29**(2), 135-154.